Journal of Computational and Applied Mathematics 353 (2019) 38–48

Contents lists available at ScienceDirect

Journal of Computational and Applied Mathematics

journal homepage: www.elsevier.com/locate/cam

An unconditionally energy stable second order finite element method for solving the Allen–Cahn equation

Congying Li [a,c], Yunqing Huang [b], Nianyu Yi [a,*]

[a] Hunan Key Laboratory for Computation and Simulation in Science and Engineering, School of Mathematics and Computational Science, Xiangtan University, Xiangtan 411105, Hunan, PR China
[b] Key Laboratory of Intelligent Computing & Information Processing of Ministry of Education, School of Mathematics and Computational Science, Xiangtan University, Xiangtan 411105, Hunan, PR China
[c] School of Mathematics and Computational Science, Huaihua University, Huaihua 418000, Hunan, PR China

ARTICLE INFO

Article history:
Received 31 January 2018
Received in revised form 24 August 2018

MSC:
65N15
65N30
65N50

Keywords:
Allen–Cahn equation
Finite element method
Energy stable
Error estimation

ABSTRACT

In this paper, we design, analyze and numerically validate an unconditionally energy stable second order numerical method for solving the Allen–Cahn equation which represents a model for anti-phase domain coarsening in a binary alloy. The proposed scheme inherits the property of the decrease of the total energy from the Allen–Cahn equation. An error estimate for the fully discretized scheme is also established. Numerical examples are presented to confirm the accuracy, efficiency, and stability of the proposed method. In particular, the method is shown to be unconditionally energy stable and second order accurate in both time and space discretizations.

1. Introduction

We consider in this paper the numerical approximation of the Allen–Cahn equation

$$\frac{\partial u}{\partial t} - \epsilon \triangle u + f(u) = 0, \qquad (x, t) \in \Omega \times (0, T], \tag{1.1}$$

with the initial condition

$$u(x, 0) = u_0(x), \qquad x \in \Omega, \tag{1.2}$$

and the homogeneous Dirichlet boundary condition:

$$u(x, t) = 0, \qquad x \in \partial\Omega, \tag{1.3}$$

where Ω is a bounded convex domain with Lipschitz boundary $\partial\Omega$, $T > 0$ is a fixed constant. The positive parameter ϵ which usually stands for the inter-facial width is a small constant compared to the characteristic length of the laboratory scale. The function $u(x, t)$ is a distribution function of the concentration for one of the two metallic components of the alloy. The reaction term $f(u) = F'(u)$ with $F(u) = \frac{1}{4}(u^2 - 1)^2$ is a given energy potential which drives the solution into the two

* Corresponding author.
E-mail addresses: lcy1869@126.com (C. Li), huangyq@xtu.edu.cn (Y. Huang), yinianyu@xtu.edu.cn (N. Yi).

https://doi.org/10.1016/j.cam.2018.12.024
0377-0427/

pure states $u = \pm 1$. As we all know that the Allen–Cahn equation is the L^2-gradient flow of the following total free energy functional

$$E(u) = \int_\Omega \left(\frac{\epsilon}{2}|\nabla u|^2 + F(u)\right) dx. \tag{1.4}$$

If we take the inner product for Eq. (1.1) with u_t, we can obtain the following equality

$$(u_t, u_t) + \varepsilon(\nabla u, \nabla u_t) + (u^3, u_t) - (u, u_t) = 0,$$

and it is easy to show that

$$\frac{dE(u(t))}{dt} = \int_\Omega \varepsilon \nabla u \nabla u_t + (u^3 - u)u_t dx = -(u_t, u_t) \le 0,$$

which means the Allen–Cahn equation possesses energy-decay property: the total energy is decreasing in time, and the following energy law holds:

$$E(u(t_2)) \le E(u(t_1)), \qquad \forall t_1 < t_2 \in (0, T]. \tag{1.5}$$

The Allen–Cahn equation was originally introduced by Allen and Cahn in [1] as a phenomenological model for antiphase domain coarsening in a binary alloy. It has been widely applied to various problems such as crystal growth [2–5], phase transitions [6,7], image analysis [8–11], grain growth [12–16], and interfacial dynamics in material science [17,18]. The decreasing of the total energy $E(u)$ of Allen–Cahn equation is considered fundamental to their derivation, their behavior and their discretization. For the Allen–Cahn equation, numerical methods inheriting the property of the decrease of the total energy are often advantageous.

During the past two decades, a great deal of mathematical effort has been devoted to the study of numerical solutions for the Allen–Cahn equation [3,15,19–30]. In [22] Feng and Prohl established some useful a priori error estimates for both semi-discrete scheme and fully discrete scheme for the Allen–Cahn equation. Optimal order and quasi-optimal order error bounds were shown for the above two schemes. A posteriori error estimates of residual type for finite element approximations of the Allen–Cahn equation were developed by Feng and Wu in [23]. Based on the proposed a posteriori error estimator, they constructed an adaptive algorithm for numerical solution of the Allen–Cahn equation. Moreover, all the error bounds in [22,23] depended on ε^{-1} only in some low polynomial order instead of exponential order. In the work by Lee and Lee [26], a simple and stable second order operator splitting method was proposed which decomposed the Allen–Cahn equation into three subequations. To achieve the second order accuracy and stability, the three subequations should be combined in proper order. In the last years, many time-stepping methods were proposed for the Allen–Cahn and Cahn–Hilliard models [31–34].

Here we especially refer to the work of Eyre [21], in which a first-order accurate nonlinearly energy stable time-stepping method for phase field models was developed, it has served as an inspiration for many other energy stable schemes. For example, Shen and Yang [30] designed stabilized first-order and second-order semi-implicit schemes which are all energy stable. They also established error estimates for two fully discrete schemes with a spectral-Galerkin approximation in space. In [20] Choi, Lee and Kim proposed an unconditionally gradient stable scheme for solving the Allen–Cahn equation, they also described its properties such as the total energy decrease and the boundedness of the numerical solution. In [3] Feng et al. constructed the energy stable first- and second-order implicit-explicit schemes with parameters for solving the Allen–Cahn equation, in which they used an implicit scheme for the diffusion term and an explicit scheme for the reaction term. The key idea is to find the feasible range of parameters involving in the IMEX schemes so that the property like (1.5) is satisfied. In [35], Zhang and Du investigated several time-stepping schemes which can maintain numerical stability and accuracy. In this work, we shall consider a second order scheme which preserves a strict energy decreasing law of the Allen–Cahn equation. The proposed numerical method uses linear finite element for spatial discrete and midpoint approach for time integration, which makes it unconditionally stable. We show the well posedness of the fully discrete scheme and derive a priori error estimation of both time and space discretizations.

The rest of the paper is organized as follows. In Section 2, we consider the finite element method for solving the Allen–Cahn equation and we show that the second order implicit scheme is unconditionally energy stable. In Section 3, we derive an error estimate for the fully discrete scheme. We then present some numerical examples in Section 4 for illustrating the accuracy and effectiveness of the proposed scheme. Finally, conclusions are drawn in Section 5.

2. Finite element scheme

For a domain $\Omega \in R^d$ we denote by $\|\cdot\|$ the norm in $L^2 = L^2(\Omega)$ and by $\|\cdot\|_k$ that in the Sobolev space $H^k = H^k(\Omega) = W^{k,2}(\Omega)$. The Sobolev space H_0^1 is defined by

$$H_0^1 = \{v \in H^1(\Omega) : v|_{\partial\Omega} = 0\}.$$

We also denote the norm in the L^∞ by $\|\cdot\|_\infty$.

Let $\mathcal{T}_h$ be a shape regular triangulation of Ω and let S_h be the corresponding finite dimensional space of piecewise linear continuous functions on Ω :

$$S_h = \{v \in H^1(\Omega) : v|_\tau \in P_1(\tau), \forall \tau \in \mathcal{T}_h\}.$$

We also denote $S_h^0 = S_h \cap H_0^1(\Omega)$.

We subdivide the time interval $[0, T]$ into a partition of N subintervals whose endpoints are denoted by $0 = t^0 < t^1 < \cdots < t^N = T$. For simplicity, we use the uniform mesh for temporal discretization. Let Δt be the time step with $t^n = n\Delta t$. And let u_h^n be the approximation of the exact solution $u(t^n)$ in the corresponding finite element space.

The weak formulation of the problem (1.1)–(1.3) reads: Find $u \in C^1(0, T; H_0^1(\Omega))$ such that

$$(u_t, v) + \epsilon(\nabla u, \nabla v) + (u^3, v) - (u, v) = 0, \qquad \forall v \in H_0^1(\Omega). \tag{2.1}$$

The corresponding semi-discrete scheme reads: Find $u_h \in C^1(0, T; S_h^0)$ such that

$$\begin{cases} (u_{h,t}, v_h) + \epsilon(\nabla u_h, \nabla v_h) + (u_h^3, v_h) - (u_h, v_h) &= 0, \qquad \forall v_h \in S_h^0, \\ u_h(0) &= u_h^0, \end{cases} \tag{2.2}$$

where u_h^0 is an approximation of u_0 in S_h^0.

Theorem 2.1 ([36]). *Let u_h and u be the solutions of (2.2) and (1.1)–(1.3), respectively. Then, for $u \in C^2(0, T; H^2(\Omega) \cap H_0^1(\Omega))$, we have*

$$\|u_h - u(t)\| \le C\|u_h^0 - u_0\| + C(u)h^2. \tag{2.3}$$

It is well known that the use of explicit scheme in time direction imposes some time-step restrictions and usually does not possess a strict energy decreasing law. We then develop a second-order scheme, unconditionally stable for the Allen–Cahn equation, given by

$$\begin{cases} \left(\dfrac{u_h^n - u_h^{n-1}}{\Delta t}, v_h\right) + \epsilon\left(\nabla \widehat{u_h^n}, \nabla v_h\right) + \left(f_h^n - \widehat{u_h^n}, v_h\right) = 0, \qquad \forall v_h \in S_h^0, \\ (u_h^0 - u_0, v_h) = 0, \qquad \forall v_h \in S_h^0. \end{cases} \tag{2.4}$$

where $\widehat{u_h^n}$ and f_h^n are defined as following

$$\begin{aligned} \widehat{u_h^n} &= \frac{u_h^n + u_h^{n-1}}{2}, \\ f_h^n &= \frac{(u_h^n)^3 + (u_h^n)^2 u_h^{n-1} + u_h^n (u_h^{n-1})^2 + (u_h^{n-1})^3}{4}. \end{aligned} \tag{2.5}$$

The approximation (2.5) for discrete the nonlinear term $f(u) = u^3 - u$ has also been introduced in Du and Nocolaides [37], and Furihata [38] for the Cahn–Hilliard equation in one dimension. They show that the corresponding scheme inherits the decrease of the total energy of the equation. And in one dimension case, the decrease of the total energy implies boundedness of discretized Sobolev norm of the solution. This in turn implies the boundedness of max norm of the solution when applying $H^1(\Omega) \hookrightarrow L^\infty(\Omega)$, and hence the unique solvability of the full discrete scheme. But the $H^1(\Omega) \hookrightarrow L^\infty(\Omega)$ is not valid for the two and three dimensions, so we cannot derive the unique solvability of scheme (2.4) following the way of [37,38].

Taking $v_h = u_h^n - u_h^{n-1}$ in (2.4) we obtain

$$\frac{\|u_h^n - u_h^{n-1}\|^2}{\Delta t} + E(u_h^n) - E(u_h^{n-1}) = 0, \tag{2.6}$$

which implies that the proposed finite element scheme (2.4)–(2.5) maintains the discrete energy decreasing property.

Theorem 2.2. *The scheme (2.4) is unconditionally energy stable and its solution satisfies*

$$E(u_h^n) \le E(u_h^{n-1}), \qquad \forall n \ge 1. \tag{2.7}$$

Theorem 2.3. *Under the time constraint $\Delta t < 2$, There exists a unique solution of the scheme (2.4)–(2.5).*

Proof. Based on the scheme (2.4), we define the following functional:

$$\begin{aligned} J(u_h^n) := &\left(\frac{1}{2\Delta t} - \frac{1}{4}\right)\int_\Omega (u_h^n)^2 - \left(\frac{1}{\Delta t} + \frac{1}{2}\right)\int_\Omega u_h^n u_h^{n-1} + \frac{\epsilon}{4}\int_\Omega |\nabla u_h^n|^2 + \frac{\epsilon}{2}\int_\Omega \nabla u_h^n \cdot \nabla u_h^{n-1} \\ &+ \frac{1}{4}\int_\Omega \left(\frac{1}{4}(u_h^n)^4 + \frac{1}{3}(u_h^n)^3 u_h^{n-1} + \frac{1}{2}(u_h^n)^2 (u_h^{n-1})^2 + u_h^n (u_h^{n-1})^3\right). \end{aligned} \tag{2.8}$$

Take the derivative of the functional $J(u_h^n)$, and for any $v_h \in S_h^0$ we have

$$\left(\frac{\delta J(u_h^n)}{\delta u_h^n}, v_h\right) = \left(\frac{1}{\Delta t} - \frac{1}{2}\right)\int_\Omega u_h^n v_h - \left(\frac{1}{\Delta t} + \frac{1}{2}\right)\int_\Omega u_h^{n-1} v_h + \frac{\epsilon}{2}\int_\Omega \nabla u_h^n \cdot \nabla v_h + \frac{\epsilon}{2}\int_\Omega \nabla u_h^{n-1} \cdot \nabla v_h + \frac{1}{4}\int_\Omega \left((u_h^n)^3 + (u_h^n)^2 u_h^{n-1} + u_h^n (u_h^{n-1})^2 + (u_h^{n-1})^3\right) v_h.$$

Rearrange it, we obtain that

$$\left(\frac{\delta J(u_h^n)}{\delta u_h^n}, v_h\right) = \left(\frac{u_h^n - u_h^{n-1}}{\Delta t}, v_h\right) + \epsilon\left(\nabla \widehat{u_h^n}, \nabla v_h\right) + \left(f_h^n - \widehat{u_h^n}, v_h\right) = 0.$$

Notice that the third and fifth terms of $J(u_h^n)$ are convex, and the second and fourth terms of $J(u_h^n)$ are linear with respect to u_h^n, so these terms are also convex. If we restrict the coefficients of the first term to be positive,

$$\frac{1}{2\Delta t} - \frac{1}{4} > 0,$$

that is $\Delta t < 2$, the corresponding functional $J(u_h^n)$ is a convex functional, and the uniqueness of the solution of scheme (2.4) is approved. □

3. Error estimates for the unconditionally energy stable scheme

In this section, we derive the error estimate of the unconditionally energy stable scheme (2.4). We shall write the error as a sum of two terms with $u^n = u(t^n)$

$$u_h^n - u^n = u_h^n - w_h^n + w_h^n - u^n = \theta^n + \rho^n, \tag{3.1}$$

where w_h^n is the elliptic projection of u^n, defined by

$$(\nabla(w_h(t) - u(t)), \nabla v) = 0, \qquad \forall v \in S_h^0. \tag{3.2}$$

Lemma 3.1 (*[36]*). *With w_h defined by (3.2) and $\rho = w_h - u$, assuming $u \in C^2(0, T; H^2(\Omega) \cap H_0^1(\Omega))$, we have*

$$\|\rho(t)\| + h\|\nabla\rho(t)\| \le C(u)h^2, \tag{3.3}$$

$$\|\rho_t(t)\| + h\|\nabla\rho_t(t)\| \le C(u)h^2, \tag{3.4}$$

where $C(u)$ is independent of h.

Lemma 3.2 (*[36]*). *Assume that $u \in C^2(0, T; H^2(\Omega) \cap H_0^1(\Omega))$. We have for the elliptic projection defined by (3.2)*

$$\|\nabla w_{h,tt}(t)\| \le C(u). \tag{3.5}$$

To derive the error estimation, we assume that there exists a positive constant C which is independent of Δt and h, such that

$$\|u_h^n\|_\infty \le C, \qquad \forall 1 \le n \le N. \tag{3.6}$$

Theorem 3.3. *Let u_h^n and $u(t^n)$ be solutions of (2.4) and (1.1)–(1.3), respectively, and suppose that u_h^n satisfies (3.6). Then, for $u \in C^2(0, T; H^2(\Omega) \cap H_0^1(\Omega))$, we have*

$$\|u_h^n - u(t^n)\| \le C\|u_h^0 - u_0\| + C(u, \varepsilon)(h^2 + \Delta t^2), \tag{3.7}$$

where u_h^0 is an approximation of u_0 in S_h^0.

Proof. From (3.1) and note that ρ_n is bounded in terms of Lemma 3.1. It remains to estimate θ^n. Denote

$$\begin{aligned} &\widehat{u_h^n} = (u_h^n + u_h^{n-1})/2, \qquad \bar{\partial} u_h^n = (u_h^n - u_h^{n-1})/\Delta t, \qquad u^{n-\frac{1}{2}} = u(t^{n-\frac{1}{2}}), \\ &f_h^n = \frac{(u_h^n)^3 + (u_h^n)^2 u_h^{n-1} + u_h^n (u_h^{n-1})^2 + (u_h^{n-1})^3}{4}, \\ &f^n = \frac{(u^n)^3 + (u^n)^2 u^{n-1} + u^n (u^{n-1})^2 + (u^{n-1})^3}{4}. \end{aligned} \tag{3.8}$$

We have

$$\begin{aligned}(\bar{\partial}\theta^n, \chi) + \varepsilon(\nabla\widehat{\theta}^n, \nabla\chi) &= (\bar{\partial}u_h^n, \chi) + \varepsilon(\nabla\widehat{u_h^n}, \nabla\chi) - (\bar{\partial}w_h^n, \chi) - \varepsilon(\nabla\widehat{w_h^n}, \nabla\chi)\\ &= \left(\widehat{u_h^n} - f_h^n, \chi\right) - (u_t^{n-\frac{1}{2}}, \chi) - (\bar{\partial}w_h^n - u_t^{n-\frac{1}{2}}, \chi)\\ &\quad - \varepsilon(\nabla w_h^{n-\frac{1}{2}}, \nabla\chi) - \varepsilon(\nabla(\widehat{w_h^n} - w_h^{n-\frac{1}{2}}), \nabla\chi)\\ &= \left(\widehat{u_h^n} - f_h^n, \chi\right) - (u^{n-\frac{1}{2}} - (u^{n-\frac{1}{2}})^3, \chi) - (\bar{\partial}w_h^n - u_t^{n-\frac{1}{2}}, \chi)\\ &\quad - \varepsilon(\nabla(\widehat{w_h^n} - w_h^{n-\frac{1}{2}}), \nabla\chi), \quad \forall\chi \in S_h^0.\end{aligned} \tag{3.9}$$

First, we consider

$$\begin{aligned}\widehat{u_h^n} - f_h^n - u^{n-\frac{1}{2}} + (u^{n-\frac{1}{2}})^3 &= \widehat{u_h^n} - u^{n-\frac{1}{2}} + (u^{n-\frac{1}{2}})^3 - f_h^n\\ &= \widehat{u_h^n} - u^{n-\frac{1}{2}} + (u^{n-\frac{1}{2}})^3 - \left(\frac{u^n + u^{n-1}}{2}\right)^3\\ &\quad + \left(\frac{u^n + u^{n-1}}{2}\right)^3 - f^n + f^n - f_h^n\\ &:= T_1 + T_2 + T_3 + T_4,\end{aligned}$$

where

$$T_1 := \widehat{u_h^n} - u^{n-\frac{1}{2}}, \qquad T_2 := (u^{n-\frac{1}{2}})^3 - \left(\frac{u^n + u^{n-1}}{2}\right)^3,$$
$$T_3 := \left(\frac{u^n + u^{n-1}}{2}\right)^3 - f^n, \quad T_4 := f^n - f_h^n.$$

Applying Lemma 3.1 we have for T_1,

$$\begin{aligned}\|T_1\| = \|\widehat{u_h^n} - u^{n-\frac{1}{2}}\| &\le \|\widehat{\theta}^n\| + \|\widehat{\rho}^n\| + \|\widehat{u}^n - u^{n-\frac{1}{2}}\|\\ &\le \|\widehat{\theta}^n\| + C(u)(h^2 + \Delta t^2).\end{aligned}$$

We estimate T_2 and T_3 as following:

$$\|T_2\| = \left\|(u^{n-\frac{1}{2}})^3 - \left(\frac{u^n + u^{n-1}}{2}\right)^3\right\| = \left\|3(\xi_1)^2\left(\frac{u^n + u^{n-1}}{2} - u^{n-\frac{1}{2}}\right)\right\| \le C(u)\Delta t^2,$$

$$\begin{aligned}\|T_3\| &= \left\|f^n - \left(\frac{u^n + u^{n-1}}{2}\right)^3\right\| = \left\|\frac{(u^n)^3 - (u^n)^2u^{n-1} - u^n(u^{n-1})^2 + (u^{n-1})^3}{8}\right\|\\ &= \left\|\frac{[(u^n)^2 - (u^{n-1})^2](u^n - u^{n-1})}{8}\right\| = \left\|\frac{(2\xi_2)(u^n - u^{n-1})^2}{8}\right\|\\ &\le C(u)\Delta t^2,\end{aligned}$$

where ξ_1 lies between $\frac{u^n+u^{n-1}}{2}$ and $u^{n-\frac{1}{2}}$, ξ_2 lies between u^n and u^{n-1}.

For the term T_4, we have

$$\begin{aligned}\|T_4\| &= \left\|f^n - f_h^n\right\|\\ &= \left\|\frac{\frac{2}{3}(u^n)^3 + \frac{1}{3}(u^n + u^{n-1})^3 + \frac{2}{3}(u^{n-1})^3 - (\frac{2}{3}(u_h^n)^3 + \frac{1}{3}(u_h^n + u_h^{n-1})^3 + \frac{2}{3}(u_h^{n-1})^3)}{4}\right\|\\ &= \frac{1}{4}\left\|\frac{2}{3}((u^n)^3 - (u_h^n)^3) + \frac{1}{3}((u^n + u^{n-1})^3 - (u_h^n + u_h^{n-1})^3) + \frac{2}{3}((u^{n-1})^3 - (u_h^{n-1})^3)\right\|\\ &\le \frac{1}{6}\|3(\xi_3)^2(u^n - u_h^n)\| + \frac{1}{12}\|3(\xi_4)^2(u^n - u_h^n)\| + \frac{1}{12}\|3(\xi_4)^2(u^{n-1} - u_h^{n-1})\|\\ &\quad + \frac{1}{6}\|3(\xi_5)^2(u^{n-1} - u_h^{n-1})\|\\ &\le C(\|u^{n-1} - u_h^{n-1}\| + \|u^n - u_h^n\|)\\ &\le C(\|\theta^n\| + \|\theta^{n-1}\|) + C(u)h^2,\end{aligned}$$

where ξ_3 lies between u^n and u_h^n, ξ_4 lies between $u^n + u^{n-1}$ and $u_h^n + u_h^{n-1}$ and ξ_5 lies between u^{n-1} and u_h^{n-1}. The existence of ξ_3, ξ_4 and ξ_5 is guaranteed by condition (3.6) and the fact that the exact solution of Allen–Cahn equation varies between -1 and 1.

Altogether the above estimates for the terms T_i, $i = 1, 2, 3, 4$ show

$$\left\| \widehat{u_h^n} - u^{n-\frac{1}{2}} \right\| \le C(\|\theta^n\| + \|\theta^{n-1}\|) + C(u)(h^2 + \Delta t^2). \tag{3.10}$$

$$\left\| (u^{n-\frac{1}{2}})^3 - f_h^n \right\| \le C(\|\theta^n\| + \|\theta^{n-1}\|) + C(u)(h^2 + \Delta t^2). \tag{3.11}$$

Then we turn our attention to (3.9). Setting $\chi = \widehat{\theta}^n$, notice that $(\bar{\partial}\theta^n, \widehat{\theta}^n) = \frac{1}{2}\bar{\partial}\|\theta^n\|^2$, we obtain

$$\begin{aligned}\frac{1}{2}\bar{\partial}\|\theta^n\|^2 + \varepsilon\|\nabla\widehat{\theta}^n\|^2 \le C\Big(&\|(u^{n-\frac{1}{2}})^3 - f_h^n\| + \|\widehat{u_h^n} - u^{n-\frac{1}{2}}\| \\ &+ \|\bar{\partial} w_h^n - u_t^{n-\frac{1}{2}}\| + \varepsilon\|\nabla(\widehat{w_h^n} - w_h^{n-\frac{1}{2}})\|\Big)\|\nabla\widehat{\theta}^n\|,\end{aligned}$$

where we have used Friedrichs' inequality $\|\theta^n\| \le C\|\nabla\theta^n\|$. And hence

$$\bar{\partial}\|\theta^n\|^2 \le C(\varepsilon^{-1})\left(\|(u^{n-\frac{1}{2}})^3 - f_h^n\|^2 + \|\widehat{u_h^n} - u^{n-\frac{1}{2}}\|^2 + \|\bar{\partial} w_h^n - u_t^{n-\frac{1}{2}}\|^2 + \varepsilon^2\|\nabla(\widehat{w_h^n} - w_h^{n-\frac{1}{2}})\|^2\right). \tag{3.12}$$

Finally, applying Lemma 3.1 we have

$$\|\bar{\partial} w_h^n - u_t^{n-\frac{1}{2}}\| \le \|\bar{\partial}\rho^n\| + \|\bar{\partial} u^n - u_t^{n-\frac{1}{2}}\| \le C(u)(h^2 + \Delta t^2), \tag{3.13}$$

and by Lemma 3.2 we have

$$\|\nabla(\widehat{w_h^n} - w_h^{n-\frac{1}{2}})\| \le C\Delta t \int_{t_{n-1}}^{t_n} \|\nabla\omega_{h,tt}\| ds \le C(u)\Delta t^2. \tag{3.14}$$

Substituting (3.10), (3.11), (3.13) and (3.14) into (3.12), we have

$$\bar{\partial}\|\theta^n\|^2 \le C(\varepsilon^{-1})(\|\theta^n\|^2 + \|\theta^{n-1}\|^2) + C(u, \varepsilon)(h^2 + \Delta t^2)^2.$$

From the definition of $\bar{\partial}\|\theta^n\|$ in (3.8), we get

$$\left(1 - C(\varepsilon^{-1})\Delta t\right)\|\theta^n\|^2 \le \left(1 + C(\varepsilon^{-1})\Delta t\right)\|\theta^{n-1}\|^2 + C(u, \varepsilon)\Delta t(h^2 + \Delta t^2)^2.$$

After some algebraic manipulation, we obtain

$$\|\theta^n\|^2 \le \frac{1 + C(\varepsilon^{-1})\Delta t}{1 - C(\varepsilon^{-1})\Delta t}\|\theta^{n-1}\|^2 + \frac{C(u, \varepsilon)\Delta t}{1 - C\Delta t}(h^2 + \Delta t^2)^2. \tag{3.15}$$

Then, by repeated application of (3.15), we have

$$\|\theta^n\|^2 \le q^n\|\theta^0\|^2 + C(u, \varepsilon)\frac{\Delta t}{1 - C(\varepsilon^{-1})\Delta t}\frac{1 - q^n}{1 - q}(h^2 + \Delta t^2)^2,$$

where $q = \frac{1+\tilde{C}\Delta t}{1-\tilde{C}\Delta t}$ and $\tilde{C} := C(\varepsilon^{-1})$.

Further more, when $\Delta t < \frac{1}{\tilde{C}}$, we obtain

$$\|\theta^n\|^2 \le q^n\|\theta^0\|^2 + C(u, \varepsilon)q^n(h^2 + \Delta t^2)^2,$$

where

$$q^n = \left(\frac{1 + \tilde{C}\Delta t}{1 - \tilde{C}\Delta t}\right)^{\frac{T}{\Delta t}} = \left(1 + \frac{2\tilde{C}\Delta t}{1 - \tilde{C}\Delta t}\right)^{\frac{1-\tilde{C}\Delta t}{2\tilde{C}\Delta t}\frac{2\tilde{C}T}{1-\tilde{C}\Delta t}}.$$

When taking the time step Δt small enough such that $|q^n| \le C$, we then have

$$\|\theta^n\|^2 \le C\|\theta^0\|^2 + C(u, \varepsilon)(h^2 + \Delta t^2)^2,$$

which shows

$$\|\theta^n\| \le C\|\theta^0\| + C(u, \varepsilon)(h^2 + \Delta t^2),$$

and thus completes the proof. □

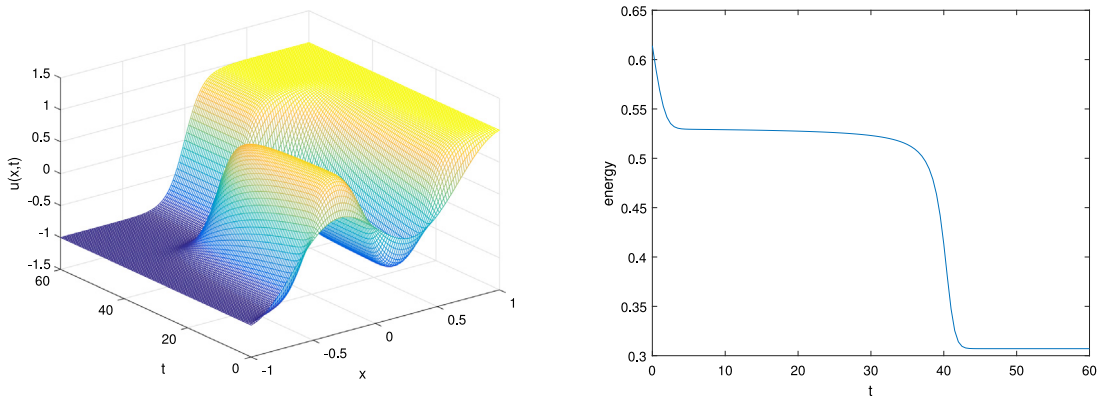

Fig. 1. Example 4.1. Left: numerical solutions with $h = \frac{1}{64}$ and $\Delta t = \frac{1}{2}$. Right: the energy evolution.

4. Numerical results

In this section, we present four numerical examples to illustrate the accuracy and the energy stable property of the proposed second order finite element scheme.

4.1. One-dimensional examples

Example 4.1. We first consider the Allen–Cahn equation

$$u_t - \epsilon u_{xx} + u^3 - u = 0, \qquad x \in [-1, 1], \tag{4.1}$$

with the initial and Dirichlet boundary conditions

$$u(x, 0) = 0.53x + 0.47 \sin(-1.5\pi x), \qquad u(-1, t) = -1, \quad u(1, t) = 1. \tag{4.2}$$

This problem has an unstable equilibrium at $u = 0$ and stable equilibria at $u = \pm 1$. One of the interesting features of this equation is the phenomenon of metastability. Regions of the solution that are near ± 1, are flat, and the interface between such areas can remain unchanged over a very long timescale before changing suddenly.

We consider the energy stable scheme (2.4) for solving the problem (4.1)–(4.2) with $\epsilon = 0.01$. Fig. 1 plots the profile of the numerical solution and the time history of the energy $E(u^n) = \int_\Omega \left(\frac{\epsilon}{2}|\nabla u|^2 + \frac{1}{4}((u^n)^2 - 1)^2\right) dx$ with $h = \frac{1}{64}$ and $\Delta t = \frac{1}{2}$. It is shown that the energy curve decreases with respect to time as the theory guaranteed.

Example 4.2. In this example, we consider the following Allen–Cahn equation

$$u_t - u_{xx} + \frac{1}{\varepsilon}(u^3 - u) = 0, \qquad (x, t) \in [0, 4] \times (0, T],$$

with the zero Neumann boundary condition

$$u_x(0, t) = u_x(4, t) = 0.$$

One of the well-known exact solutions of the Allen–Cahn equation is the traveling wave solution:

$$u(x, t) = 0.5 - 0.5 \tanh\left(\frac{x - 0.5 - st}{2\sqrt{2\epsilon}}\right),$$

where $s = 3/(\sqrt{2\epsilon})$ is the speed of the traveling wave. The initial condition is defined from the traveling wave solution at $t = 0$.

We investigate the performance of the energy stable scheme on the traveling wave problem with $\epsilon = 0.0018$ and compute $u(x, t)$ for $0 < t \le T_f = 1/s$. We first test the order of convergence of the proposed energy stable scheme. We begin to test the accuracy on the spatial discretization by fixing the time step $\Delta t = 1.0e{-}06$. The errors at time $T = T_f$ are reported in Table 1. The numerical results show that the order of convergence of the errors $\|u - u_h\|_{L^2(\Omega)}$ and $|u - u_h|_{H^1(\Omega)}$ are 2 and 1, respectively. Next we test the accuracy of the temporal discretization with a small spatial mesh size $h = 1.0e - 04$. The L^2-norm errors and corresponding convergence rates are shown in Table 2. We see clearly that the convergence rate for time discretization is 2 for the energy stable scheme. These results are in consistency with the theory established in Section 3.

Table 1
Example 4.2. Errors and convergence rate of the spatial discretization accuracy test, $\Delta t = 1.0e-06$, $T = T_f$.

h	1/16	1/32	1/64	1/128	1/256
$\|u-u_h\|_{L^2}$	4.00e−03	1.00e−03	2.52e−04	6.31e−05	1.60e−05
Order	–	2.00	1.99	2.00	1.98
$\|u-u_h\|_{H^1}$	2.22e−01	1.12e−01	5.60e−02	2.80e−02	1.40e−02
Order	–	0.99	1.00	1.00	1.00

Table 2
Example 4.2. Errors and convergence rate of the temporal discretization accuracy test, $h = 1.0e-04$, $T = T_f$.

Δt	$1.00e-04$	$5.00e-05$	$2.50e-05$	$1.25e-05$	$6.25e-06$
$\|u-u_h\|_{L^2}$	6.96e−04	1.74e−04	4.34e−05	1.08e−05	2.67e−06
Order	\	2.00	2.00	2.00	2.02

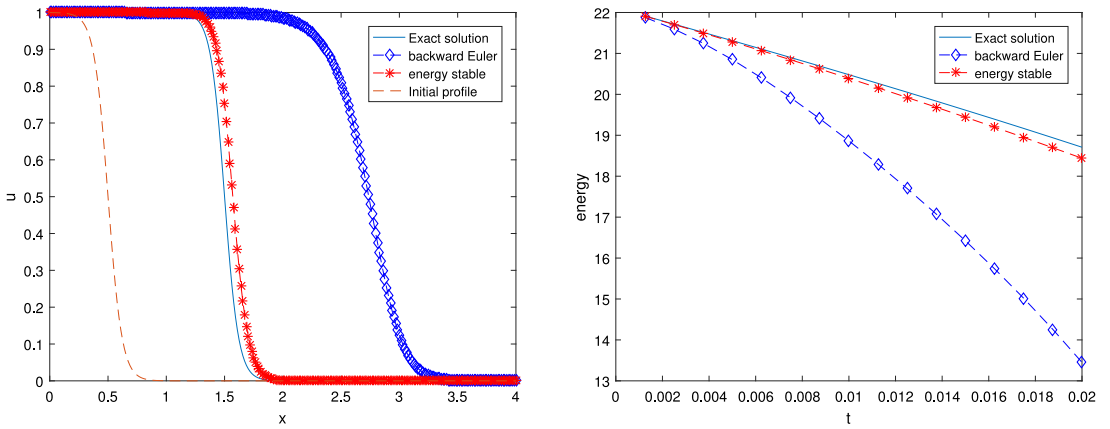

Fig. 2. Example 4.2, $h = \frac{1}{64}$ and $\Delta t = \frac{1}{800}$. Left: numerical solutions obtained by the backward Euler scheme and energy stable scheme; Right: time evolution of the discrete energy.

We also investigate the time evolution of the discrete energy

$$E(u^n) = \int_\Omega \left(\frac{1}{2}|\nabla u|^2 + \frac{1}{4\epsilon}((u^n)^2 - 1)^2 \right) dx$$

for the energy stable scheme. For comparison, we also apply the backward Euler scheme for solving this problem. Following the proof of Theorem 2.3, we obtain that under the constraint on time step $\Delta t < 2\epsilon$, the energy stable scheme admits a unique solution. Then we set $h = \frac{1}{64}$ and $\Delta t = \frac{1}{800}$. Fig. 2 plots the two numerical solutions at time $t = T_f$ obtained by the two schemes and the time history of the energy. We clearly see that the energy stable scheme induces smaller error, and the discrete energy decrease property matches well with the exact one, while the backward Euler scheme produces larger errors and the energy decreases faster.

4.2. Two-dimensional examples

Example 4.3. In the following, we consider the energy stable scheme for the Allen–Cahn equation in two dimensions,

$$\frac{\partial u}{\partial t} - \epsilon \triangle u + u^3 - u = 0, \qquad (x, y, t) \in (0, 2\pi) \times (0, 2\pi) \times (0, T],$$

with the homogeneous Dirichlet boundary condition. The initial condition is chosen such that

$$u_0(x, y) = 0.05 \sin x \cdot \sin y.$$

The parameter is chosen as $\epsilon = 0.01$.

We take the time step $\Delta t = 0.5$ and the uniform triangulations which are generated as following: partition the computational domain $\Omega = (0, 2\pi)^2$ into $N \times N$ rectangles, and then partition each rectangle into two right angled triangles. In Fig. 3 we plot the time history of the energy $E(u^n) = \int_\Omega \left(\frac{\epsilon}{2}|\nabla u|^2 + \frac{1}{4}((u^n)^2 - 1)^2 \right) dx$ and the numerical solutions at times $t = 1, 10, 60, 550, 600$, respectively. The figure shows that energy decreases with respect to time. We notice that the figure changed substantially before $t = 10$, then the figure changed slowly after $t = 10$ and became stable after $t = 550$, which coincides with the trend of the energy curve.

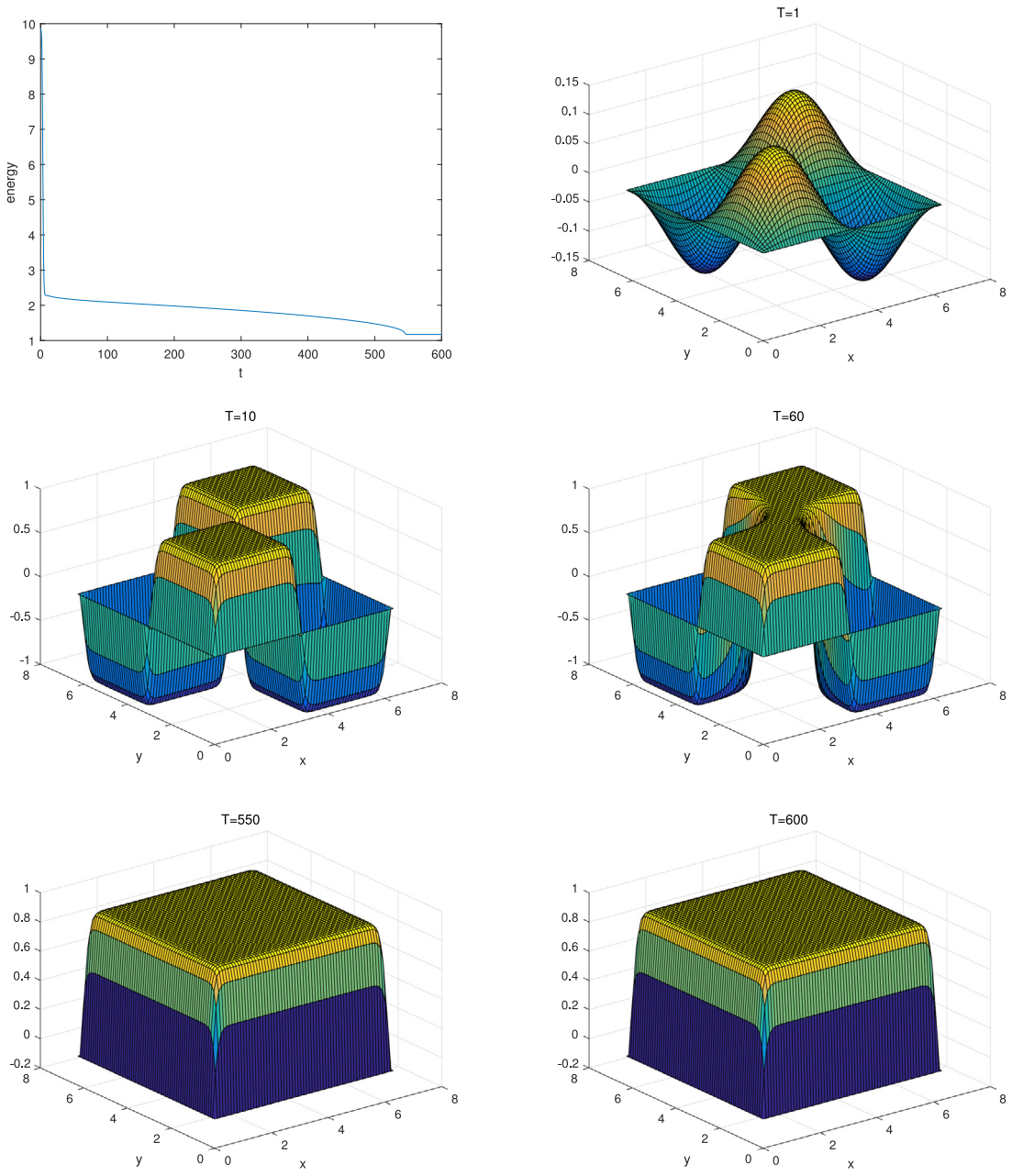

Fig. 3. Example 4.3, $N = 64$ and $\Delta t = \frac{1}{2}$, time evolution of the discrete energy and the numerical solutions at $t = 1, 10, 60, 550, 600$.

Example 4.4. In this example, numerical simulations of motion of a circle by its mean curvature are presented. We consider the Allen–Cahn equation in the following form:

$$u_t - \Delta u + \frac{1}{\varepsilon}(u^3 - u) = 0. \tag{4.3}$$

It was formally testified that, as $\epsilon \to 0$, the zero level set of u, which is denoted by

$$\Gamma_t^\epsilon := \{x \in \Omega; \qquad u(x, t) = 0\},$$

approaches a surface Γ_t that evolves according to the geometric law

$$V = -(\frac{1}{R_1} + \frac{1}{R_2}) = -\kappa, \tag{4.4}$$

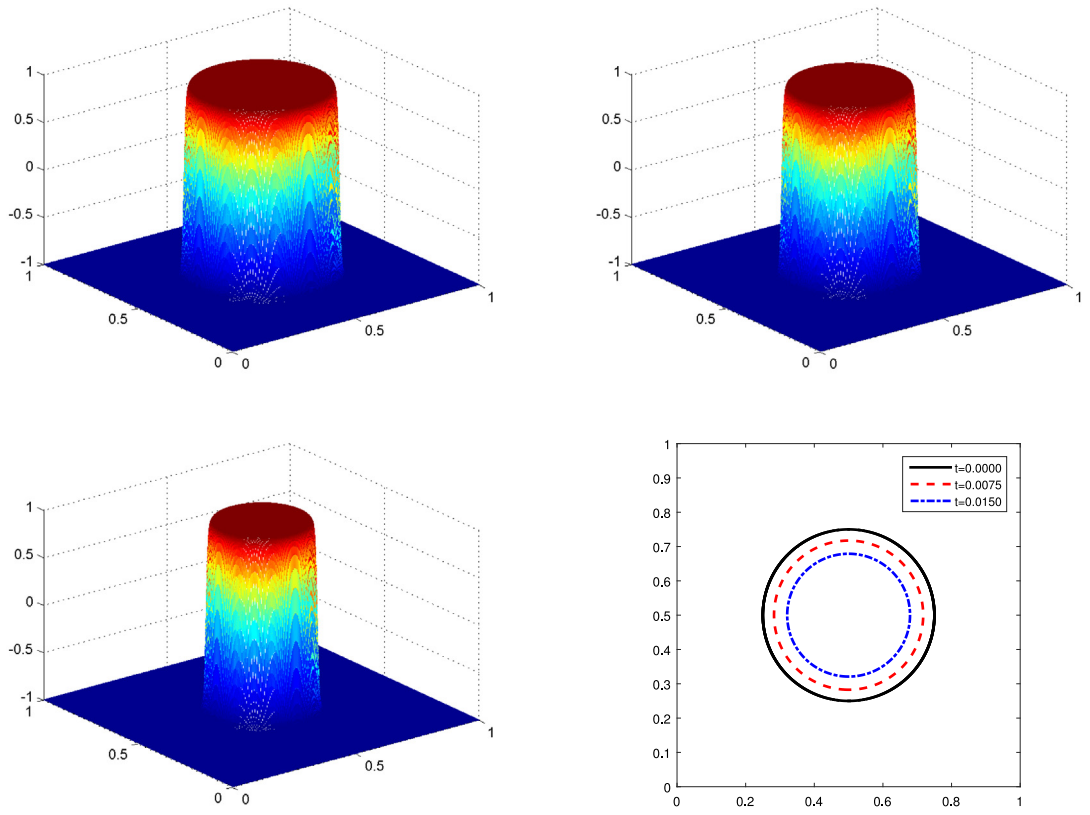

Fig. 4. Example 4.4, the evolution of the concentration $u(x, y, t)$ with the initial data given by (4.5). Top left: the concentration $u(x, y, 0)$; Top right: the concentration $u(x, y, 0.0075)$; Down left: the concentration $u(x, y, 0.015)$; Down right: the zero level contour lines of $u(x, y, t)$.

where V is the normal velocity of the surface Γ_t at each point, R_1 and R_2 are the principal radii of curvatures at the point of the surface, and κ is its mean curvature [1,39]. With a single radius of curvature in two dimensions, (4.4) becomes $V = -1/R$. If the radius of the initial circle is set to R_0 and we denote the radius at time t as $R(t)$, then $V = \frac{dR(t)}{dt} = -\frac{1}{R(t)}$. Its solution is given as

$$R(t) = \sqrt{R_0^2 - 2t}.$$

If the analytic area at time t is denoted as $A(t)$, then we have

$$A(t) = \pi(R_0^2 - 2t).$$

We numerically investigate the performance of the energy stable scheme with the initial condition

$$u(x, y, 0) = \tanh \frac{0.25 - \sqrt{(x - 0.5)^2 + (y - 0.5)^2}}{\sqrt{2}\epsilon}. \tag{4.5}$$

The computational domain $\Omega = (0, 1) \times (0, 1)$ is uniformly partitioned with a 512×512 cells and take the time step $\Delta t = 0.0001$. Fig. 4 shows the evolutions of the initial concentration $u(x, y, 0)$ given by (4.5). The zero level contour lines of the concentration $u(x, y, t)$ at time $t = 0, 0.0075, 0.015$ are also plotted in Fig. 4. The results are consistent with those reported in [27]. It is observed that the circle shrinks as the theory predicted.

5. Conclusions

In this paper, we develop an unconditionally energy stable second-order numerical method for solving the Allen–Cahn equation. We use the linear finite element method for spatial discretization and an unconditionally energy stable scheme for temporal discretization. The new scheme inherits the decrease of the total energy from the Allen–Cahn equation. An error estimate for the proposed numerical scheme is derived and the convergence order is 2 in both time and space. Finally, several numerical examples were presented to confirm the accuracy, efficiency and stability of the proposed scheme.

The Allen–Cahn and Cahn–Hilliard equations arising from the phase field models show the phenomenon of the boundary layer and an appropriate numerical method for these equations requires the spatial mesh size and time step size have to

properly relate to the interaction length ε. So it is natural to use adaptive mesh techniques so the fine meshes are only used in a small neighborhood of the phase front. We will continue our works in the following issues: (i) develop efficient and stable time stepping methods for phase field models; (ii) derive the a posteriori error estimation and design time and space adaptive methods for Allen–Cahn equation and Cahn–Hilliard equation. We will report these results and applications in our future works.

Acknowledgments

Li's research was supported by Hunan Provincial Innovation Foundation for Postgraduate, PR China (CX2016B247). Huang's research was supported by NSFC, PR China Project (91430213).Yi 's research was supported by NSFC Project, PR China (11671341) and Department of Education of Hunan Province Project, PR China (16A206).

References

[1] S.M. Allen, J.W. Cahn, A microscopic theory for antiphase boundary motion and its application to antiphase domain coarsening, Acta Metall. 27 (1979) 1085–1095.
[2] W.J. Boettinger, J.A. Warren, C. Beckermann, A. Karma, Phase-field simulation of solidification, Annu. Rev. Mater. Sci. 32 (2002) 163–194.
[3] X. Feng, H. Song, T. Tang, J. Yang, Nonlinear stability of the implicit-explicit methods for the Allen–Cahn equation, Inverse Probl. Imaging 7 (2013) 679–695.
[4] A. Karma, W.J. Rappel, Quantitative phase-field modeling of dendritic growth in two and three dimensions, Phys. Rev. E 57 (1998) 4323–4349.
[5] R. Kobayashi, Modeling and numerical simulations of dendritic crystal growty, Physica D 63 (1993) 410–423.
[6] C.M. Elliott, B. Stinner, Computation of two-phase biomembranes with phase dependent material parameters using surface finite element, Commun. Comput. Phys. 13 (2013) 325–360.
[7] Y. Li, H.G. Lee, J. Kim, A fast, robust, and accurate operator splitting method for Phase-field simulation of crystal growth, J. Cryst. Growth 321 (2011) 176–182.
[8] M. Beneš, V. Chalupecký, K. Mikula, Geometrical image segmentation by the Allen–Cahn equation, Appl. Numer. Math. 51 (2004) 187–205.
[9] S. Esedoglu, Y.H.R. Tsai, Threshold dynamics for the piecewise constant Mumford-Shan functional, J. Comput. Phys. 211 (2006) 367–384.
[10] D.A. Kay, A. Tomasi, Color image segmentation by the vector valued Allen–Cahn phase-field model: A multigrid solution, IEEE Trans. Image Process 18 (2009) 2330–2339.
[11] H.G. Lee, J. Shin, J.Y. Lee, First and second order operator splitting method for phase-field crystal equation, J. Comput. Phys. 299 (2015) 82–91.
[12] D. Fan, L.Q. Chen, Computer simulation of grain growth using a continuum field model, Acta Mater. 45 (1997) 611–622.
[13] R. Kobayashi, J.A. Warren, W.C. Carter, A continuum model of grain boundaries, Physica D 140 (2000) 141–150.
[14] C.E. Krill, L.Q. Chen, Computer simulation of 3-D grain growth using a phase-field model, Acta Mater. 50 (2002) 3057–3073.
[15] Y. Li, J. Kim, Multiphase image segmation using a phase-field model, Comput. Math. Appl. 62 (2011) 737–745.
[16] I. Steinbach, F. Pezzolla, B. Nestler, M. Seeßelberg, R. Prieler, G.J. Schmitz, J.L.L. Rezende, A phase field concept for multiphase system, Physica D 94 (1996) 135–147.
[17] L. Golubovic, A. Levandovsky, D. Moldovan, Interface dynamics and far-from-equilibrium phase transitions in multilayer epitaxial growth and erosion on crystal surfaces: Continuum theory insights, East Asian J. Appl. Math. 1 (2011) 297–371.
[18] J. Kim, Phase-field models for multi-component fluid flows, Commun. Comput. Phys. 12 (2012) 613–661.
[19] P.W. Bates, S. Brown, J. Han, Numerical analysis for a nonlocal Allen–Cahn equation, Int. J. Numer. Anal. Model. 6 (2009) 33–49.
[20] J.W. Choi, H.G. Lee, D. Jeong, J. Kim, An unconditionally gradient stable numerical method for solving the Allen–Cahn equation, Physica A 388 (2009) 1791–1803.
[21] D.J. Eyre, An unconditionally stable one-step scheme for gradient systems, 1998, unpublished article. http://www.math.utah.edu/eyer/research/methods/stable.ps.
[22] X. Feng, A. Prohl, Numerical analysis of the Allen–Cahn equation and approximation for mean curvature flaws, Numer. Math. 94 (2003) 33–65.
[23] X. Feng, H. Wu, A posteriori err estimates and an adaptive finite element method for the Allen–Cahn equation and the mean curvature flow, J. Sci. Comput. 24 (2005) 121–146.
[24] D. Jeong, S. Lee, D. Lee, J. Shin, J. Kim, Comparison study of numerical methods for solving the Allen–Cahn equations, Comput. Mater. Sci. 111 (2016) 131–136.
[25] H.G. Lee, J.Y. Lee, A semi-analytical Fourier spectral method for the Allen–Cahn equation, Comput. Math. Appl. 68 (2014) 174–184.
[26] H.G. Lee, J.Y. Lee, A second order operator splitting method for Allen–Cahn type equations with nonlinear source terms, Physica A 432 (2015) 24–34.
[27] Y. Li, H.G. Lee, D. Jeong, J. Kim, An unconditionally stable hybrid numerical method for solving the Allen–Cahn equation, Comput. Math. Appl. 60 (2010) 1591–1606.
[28] H. Ramanarayan, T.A. Abinandanan, Spinodal decomposition in poly-crystalline alloys, Physica A 318 (2003) 213–219.
[29] H. Song, L. Jiang, Q. Li, A reduced order method for Allen–Cahn equations, J. Comput. Appl. Math. 292 (2016) 213–229.
[30] J. Shen, X. Yang, Numerical approximations of Allen–Cahn and Cahn–Hilliard equations, Discrete Contin. Dyn. Syst. 28 (2010) 1669–1691.
[31] F. Guillén-González, G. Tierra, Second order schemes and time-step adaptivity for Allen–Cahn and Cahn–Hilliard models, Comput. Math. Appl. 68 (2014) 821–846.
[32] F. Luo, T. Tang, H. Xie, Parameter-free time adaptivity based on energy evolution for the Cahn–Hilliard equation, Commun. Comput. Phys. 19 (2016) 1542–1563.
[33] J. Shen, J. Xu, J. Yang, The scalar auxiliary variable (SAV) approach for gradient flows, J. Comput. Phys. 353 (2018) 407–416.
[34] L. Zhu, Efficient and stable exponential Runge–Kutta methods for parabolic equations, Adv. Appl. Math. Mech. 9 (2017) 157–172.
[35] J. Zhang, Q. Du, Numerical studies of discrete approximations to the Allen–Cahn equation in the sharp interface limit, SIAM J. Sci. Comput. 31 (2009) 3042–3063.
[36] V. Thomée, Galerkin Finite Element Methods for Parabolic Problems, second ed., Springer, 2006.
[37] Q. Du, R.A. Nicolaides, Numerical analysis of a continuum model of phase transition, SIAM J. Numer. Anal. 28 (1991) 1310–1322.
[38] D. Furihata, A stable and conservative finite difference scheme for the Cahn–Hilliard equation, Numer. Math. 87 (2001) 675–699.
[39] W. Bao, Approximation and comparison for motion by mean curvature with intersection point, Comput. Math. Appl. 46 (2003) 1211–1228.